J. CUMIN, D. NOVOSELOVIĆ, M. SAMARDŽIĆ, IVA SAMARDŽIĆ

ISSN 0543-5846
METABK 62(3-4) 391-393 (2023)
UDC – UDK 669.15.26.24:620.16:539.374:51.086.5:31.517=111

STATISTICAL ANALYSIS OF DIFFERENT MATHEMATICAL MODELS FOR STRESS-STRAIN CURVES OF AISI 321 STAINLESS STEEL

Received – Primljeno: 2023-03-02
Accepted – Prihvaćeno: 2023-04-25
Original Scientific Paper – Izvorni znanstveni rad

This paper presents statistical analysis of data obtained by uniaxial tensile testing of AISI 321 stainless steel. This data is required as material input in numerical software, such as Abaqus, Ansys, MSC Marc, Nastran, etc. This data can be provided in the software as a set of points (piecewise linear model) that is cumbersome to enter, or it can be provided as a mathematical model, in the case of which the Finite Element Method (FEM) software calculates desired points directly from the mathematical model. Various mathematical models can be used to approximate tensile test data depending on the material loading state (linear, elasto-plastic, plastic). In this paper, the same uniaxial test data is analyzed, and curve fitting parameters are shown for each mathematical model.

Key words: AISI 321, true stress, true strain, mathematical model, statistical analysis

INTRODUCTION

The tensile test results are often given as a large set of data plotted in engineering stress-strain diagram, as shown in Figure 1. The tensile testing norm ISO 6892-1 for metallic materials gives definition of yield strength R_e / MPa, proof strength at plastic extension $R_{p0,2}$ / MPa, yield strength R_m / MPa, percentage elongation θ / %, and percentage reduction Z / %, all of which are used in the engineering practice as indication of general material mechanical properties.

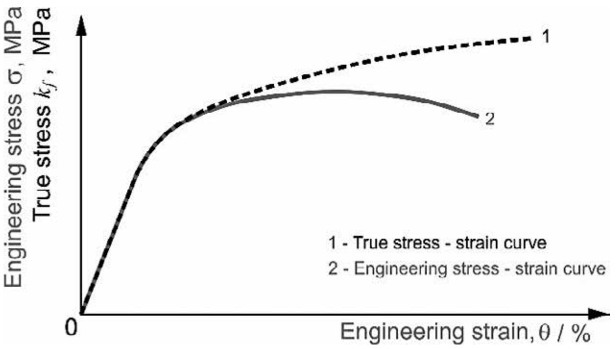

Figure 1 Engineering and true stress-strain curves

Finite element method-oriented software requires data input as true stress (k_f / MPa) vs. true strain (φ) values, which are calculated in a different way (1).

$$k_f = \frac{F}{A} \text{ / MPa} \quad (1)$$

where A - current surface of specimen / mm^2.

Engineering stress (2) is calculated with respect to initial specimen surface A_0 and from here, the difference among stress strain curves can be seen in Figure 1.

$$\sigma = \frac{F}{A_0} \text{ / MPa} \quad (2)$$

The data of true stress-true strain can be appropriately described by Ludwik-Hollomon power function (3).

$$k_f = C \cdot \varphi^n \text{ / MPa} \quad (3)$$

This function is usually used in theoretical and practical description of parameters in metal forming processes, as described in available literature [1-3].

Swift mathematical function (4) is also frequently used [1]:

$$k_f = C\left(\varphi_o + \varphi\right)^n \text{ / MPa} \quad (4)$$

This model deals separately with strains that appear in elastic region (φ_0), as well as with strains in the plastic region (φ).

The Voce model is usually used for isotropic strain hardening of materials (5) [1, 4]. This model is usable for high material plasticity and low strain-hardening.

$$k_f = \sigma_s + R_0 \cdot \varphi + R_{inf}\left(1 - e^{-b\cdot\varphi}\right) \text{ / MPa} \quad (5)$$

where σ_s - elasticity limit / MPa; R_0, R_{inf}, b - fitting parameters of the model.

For complex material behavior, the coupled Swift-Voce model can be used (6) [1]:

$$k_f = (1-\alpha)C\left(\varphi_0 + \varphi\right)^n + \alpha\left[\sigma_s + R_0 \cdot \varphi + R_{inf}\left(1 - e^{-b\cdot\varphi}\right)\right] \quad (6)$$

where a is measure of contribution of Swift or Voce models (i.e. a = 1 → pure Swift model; a = 0 → pure Voce model).

J. Cumin (jcumin@unisb.hr), D. Novoselović, M. Samardžić, Iva Samardžić, Mechanical Engineering Faculty in Slavonski Brod, University of Slavonski Brod, Croatia.

Finite element software like MSC Marc requires data set to be entered as a true stress-true plastic strain function, thus true strain needs to be disassembled to elastic strain $\varphi^{e}_{i,j}$, and plastic strain $\varphi^{p}_{i,j}$ (7) [5]:

$$\varphi_{i,j} = \varphi^{e}_{i,j} + \varphi^{p}_{i,j} \tag{7}$$

In order to obtain this data set, it is necessary to process true stress-true strain data, as follows (8):

$$\varphi_p = \varphi - \frac{k_f}{E} \tag{8}$$

MATERIAL

The tensile test results are often given as a large set of data. From AISI 321 (X6CrNiTi18-10 / EN 1.4541) [6], the tensile test specimens were cut according to EN norm ISO 6892-1, as shown in Figure 2.

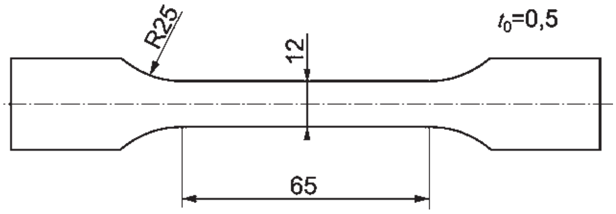

Figure 2 Tensile test specimen; ISO 6892-1

Figure 3 shows true stress-true strain data obtained with the Shimadzu AGS-X 10 kN tensile testing machine.

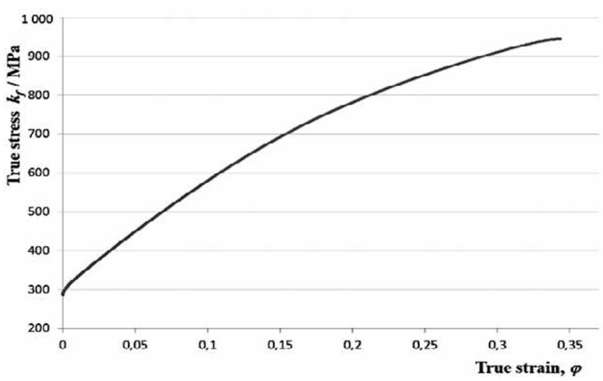

Figure 3 True stress vs. true strain on AISI 321 tensile test specimens

The most finite element software requires input of material data, and some of them offer data fitting options. Since "piecewise linear" is offered, the user can input selected points on the diagram and the software interpolates values. However, since it uses linear extrapolation method, the residuals exist between measured data and used data in the software, which leads to accumulated errors. Moreover, the input of large amount of data points is cumbersome (the data from Figure 3 consists of approximate 5 000 sampled data points). To overcome this problem, the data needs to be processed by nonlinear regression models for best fit.

MATHEMATICAL MODELS

After nonlinear regression analysis the four applicable mathematical models were obtained.

a) Hollomon model

The obtained mathematical model (best fit) is given by (9):

$$k_f = 1\,190,08 \cdot \varphi^{0,288422} \tag{9}$$

The coefficient of determination R^2, estimated variance for data fitting σ^2, and standard deviation σ are given in Table 1.

Table 1 **Hollomon model parameters**

Hollomon model	$k_f = 1190,08 \cdot \varphi^{0,288422}$ $\sigma = 11,37$; $\sigma^2 = 129,27$; $R^2 = 0,99607$)			
	Estimate	Standard error	*t*-statistic	*p* - value
C	1 190,08	5,00083	237,98	$2,20255 \cdot 10^{-2\,564}$
n	0,288422	0,00177	162,46	$5,18115 \cdot 10^{-1\,893}$

b) Ludwik model

The obtained mathematical model (best fit) (10) is given by a variant of equation (3):

$$k_f = 273,792 + 1\,544,37 \cdot \varphi^{0,705549} \tag{10}$$

The coefficient of determination R^2, estimated variance for data fitting σ^2, and standard deviation σ are given in Table 2.

Table 2 **Ludwik model parameters**

Ludwik model	$k_f = 273,792 + 1544,37 \cdot \varphi^{0,705549}$ $\sigma = 60,56$; $\sigma^2 = 3667,93$; $R^2 = 0,98887$)			
	Estimate	Standard error	*t*-statistic	*p* - value
k_{f0}	273,792	0,5136	533,01	$1,53678 \cdot 10^{-4\,091}$
C	1 544,37	3,1305	493,32	$1,43168 \cdot 10^{-3\,941}$
n	0,705549	0,00159	441,28	$1,39498 \cdot 10^{-3\,726}$

c) Swift model

The obtained mathematical model (best fit) (11) is given by equation (4):

$$k_f = 1\,252,19 + (0,002 + \varphi)^{0,315633} \tag{11}$$

d) Voce model

The obtained mathematical model (best fit) (12) is given by equation (5):

$$k_f = 285 + 85,059 \cdot \varphi + 824,86\left(1 - e^{-4,33129 \cdot \varphi}\right) \tag{12}$$

Table 3 **Swift model parameters**

Swift model	$k_f = 1252,19 + (0,002 + \varphi)^{0,315633}$ ($\sigma = 43,13$; $\sigma^2 = 1860,02$; $R^2 = 0,99435$)			
	Estimate	Standard error	*t*-statistic	*p* - value
C	1 252,19	3,8054	329,06	$4,14067 \cdot 10^{-3\,167}$
n	0,315633	0,001308	241,34	$4,94790 \cdot 10^{-2\,590}$

Table 4 **Voce model parameters**

Voce model	$k_f = 285 + 85,059 \cdot \varphi + 824,86\,(1 - e^{-4,33129 \cdot \varphi})$ $\sigma = 5,33$; $\sigma^2 = 28,413$; $R^2 = 0,99991$)			
	Estimate	Standard error	*t*-statistic	*p* - value
R_o	85,0591	35,4947	2,39639	$1,65979 \cdot 10^{-2}$
R_{inf}	824,86	21,3265	38,6777	$4,51487 \cdot 10^{-283}$
b	4,33129	0,074503	58,1359	$7,831844 \cdot 10^{-551}$

Table 3 shows Swift model parameters (11), and Table 4 shows Voce model (12) parameters.

Figure 4 shows fitted mathematical models and measured tensile test data of the samples. All models are similar and provide decent fitting, yet the best approximation is made by the Voce model (5, 12). The Swift-Voce model was also used, but it resulted in a very complex expression with minimal difference from the Voce model itself, so it is not described in this paper. It has been shown in [7] that even more complex mathematical models can be used for good approximation of true stress-true strain curves, but they are cumbersome for programming in FEM software.

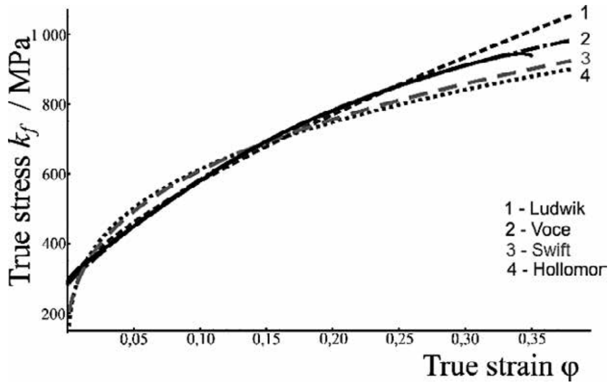

Figure 4 Comparison of measured tensile test data and fitted mathematical models

The fitting of the applied models is best seen on the diagram of residuals Δ (13), Figure 5.

$$\Delta = k_f\left(\varphi\right)_{data} - k_f\left(\varphi\right)_{model} \tag{13}$$

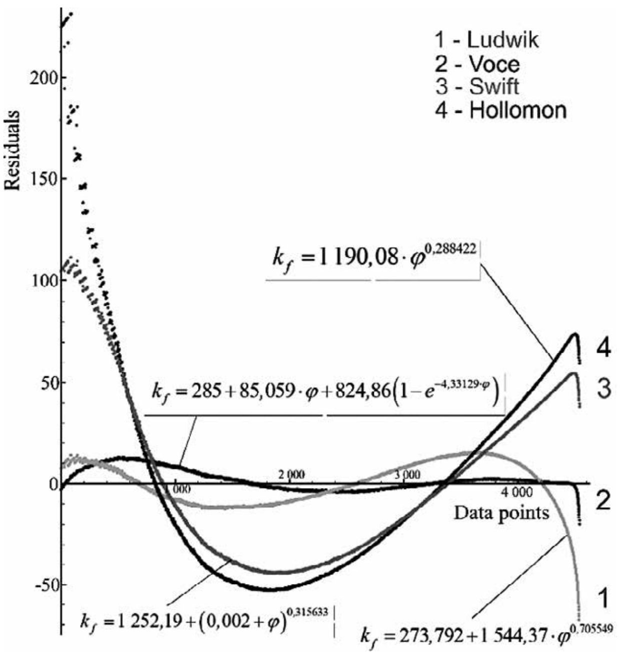

Figure 5 Residuals for the used mathematical functions

CONCLUSION

The uniaxial tensile test data fitting is presented in this paper. Description of stress-strain relations for different materials, as well as for the tested AISI 321 (X6CrNiTi18-10 / EN 1.4541) steel material can be found in the literature. It is common to approximate material properties in some range. Statistical methods are used when close approximation of the material data is required (for example, finite element simulation). This paper overviews the most common mathematical models used for true stress-true strain relations. This research confirmed that the Voce model (12) provided the best overall fitting for the tested material AISI 321, as clearly visible in Figures 4 and 5. The usage of combined Swift-Voce model (6) proved to be cumbersome for data fitting, since clear parametric factors could barely be obtained, and even then, just a minor difference from the Voce model (12) was observed. For this reason, such model was not included in the statistical analysis.

REFERENCES

[1] R. Chales, A.S.M. Cardoso, J.M. Pardal, S.S.M. Tavares, M.M. Silva, D.A.P. Reis: Modeling and Numerical Validation of Stress-Strain Curves of Maraging Steels, Grades 300 and 350 Under Hydrogen Embrittlement, Materials Research 24 (2021) 3, 1-11

[2] A. Rajeshkannan, S. Narayan, A. Jeevanantham: Modelling and analysis of strain hardening characteristics of sintered steel preforms under cold forging, AIMS Materials Science 6 (2019) 1, 63-79

[3] A. Chukanov, A. Gvozdev, A. Sergeev, S. Kutepov, P. Medvedev, D. Maliy, A. Yakovenko, I. Shiroky: Historical aspects of mathematical analysis of metal material deformation diagrams, Chebyshevskii 20 (2019) 1, 405-423

[4] E. Arslan, M. Zigo, G. Kepplinger: A Novel Approach for Determination of Hardening Parameters of an Aluminum Alloy under Cyclic Loading with High Amplitudes, IOP Conference Series, Materials Science and Engineering 947 (2020), 1-5

[5] V. Okorokov, Y. Gorash, D. Mackenzie, R. Rijswick: New Formulation of Nonlinear Kinematic Hardening Model, Part I: A Dirac Delta Function Approach, International Journal of Plasticity 122 (2019), 89-114

[6] D. Maric, J. Cumin, T. Solic, I. Samardzic: Quality Analysis of AISI 321 Welds of Bellow Compensators Used in Shipbuilding, Journal of Marine Science and Engineering 10 (2022) 4, 452

[7] W. Grzesik, P. Niesłony, P. Laskowski: Determination of Material Constitutive Laws for Inconel 718 Superalloy Under Different Strain Rates and Working Temperatures, Journal of Materials Engineering and Performance 26 (2017), 5705-5714

Note: Responsible person for English translation: Martina Šuto